Astron. & Astrophys. 36, 69—78 (1974)

Steady and Oscillatory $\alpha\omega$-dynamos

W. Deinzer, H.-U. v. Kusserow and M. Stix
Universitäts-Sternwarte Göttingen

Received July 27, 1974

Summary. Using the model of Deinzer and Stix (1971) of an $\alpha\omega$-dynamo we investigate the problem whether the preferred magnetic field mode is steady or oscillatory for any particular strength and spatial distribution of the induction effects (α-effect and non-uniform rotation). We find that a spatial separation of these two effects favours the steady modes, in contrast to an earlier assertion of Steenbeck and Krause (1969a). The steady modes have dipoletype symmetry if the dynamo-number is positive, and quadrupoletype symmetry if the dynamo number is negative. The possible relevance of the steady dipole solutions to the dynamo operating in the Earth's interior is discussed.

Key words: dynamo — α-effect — differential rotation — geomagnetism

I. Introduction

It has been suggested by several authors (Parker, 1955; Steenbeck and Krause, 1969a; Deinzer and Stix, 1971; Roberts and Stix, 1972; Köhler, 1973) that the mean magnetic field of the Sun governing the 22-year cycle is an oscillatory solution of an "$\alpha\omega$-dynamo": Non-uniform rotation creates toroidal magnetic flux from poloidal field components, and the "α-effect", an e.m.f. $\alpha\boldsymbol{B}$ parallel to the mean field existing in cyclonic convection, causes toroidal currents to flow and so to regenerate the poloidal field.

Are $\alpha\omega$-dynamos always oscillatory, or do steady solutions also exist? Or, more precisely, which type of solution is "dominant" (or "preferred") in a particular model in the sense that it is marginally stable for *smaller* values of the relevant magnetic Reynolds numbers? Parker (1971) has argued that steady solutions are preferred when the dynamo consists of a full sphere or a thick spherical shell such as the liquid core of the Earth; oscillatory modes should dominate in a thin spherical shell dynamo such as the solar convection zone. Roberts (1972) computed solutions of a number of $\alpha\omega$-dynamos and found that oscillatory solutions were dominant even in dynamos occupying a full sphere; they could however be made steady by means of a (sufficiently strong) meridional circulation. Stix (1973) found that the dynamo model of Levy (1972a) has both steady and oscillatory solutions; which of these is preferred depends on the exact position of the rings of cyclones in Levy's model and on the sign of the "dynamo number"

$$P = R_\alpha R_\omega = \frac{\alpha_0 R}{\eta} \cdot \frac{\Delta\omega R^2}{\eta},$$

where α_0 is a characteristic value of α in the northern hemisphere, $\Delta\omega$ is the total amount of differential rotation, R is the radius of the sphere and η is the (turbulent) magnetic diffusivity which in our models will be treated as a constant. In the most often investigated case only two magnetic Reynolds numbers, R_α and R_ω, are relevant, and the frequencies and growth rates of the solutions solely depend on their product, P.

The models mentioned above show that in order to obtain oscillatory solutions with mean fields migrating from the poles toward the equator we must require that $P<0$. With this sign of P Levy's model has preferred oscillatory solutions if the induction effects are confined to the outer third of the sphere. When $P>0$, however, the model favours the steady mode irrespective of the positions of the induction effects (Stix, 1973). Thus, the situation is still not clear; we shall therefore investigate the question of oscillatory versus steady solutions further, using the model of Deinzer and Stix (1971; we shall refer to this article as "Paper I"). This model has the advantage of having a more realistic latitude distribution of $\alpha(\propto \cos\theta)$ than Levy's model, although the radial dependence of α and $\partial\omega/\partial r$ is still in the form of δ-functions. But this form enables us to calculate solutions for a wide range of the characteristic parameters, r_1 and r_2 (the radial position of shear and α-effect) and P, without a large expenditure of computing. We shall see in Section III how the (r_1, r_2) parameter space is divided into regions of steady and oscillatory solutions. We shall also see that, if steady solutions *are* possible, they are of dipole-type parity in the case $P>0$ and of quadrupole-type parity when $P<0$.

If $P>0$, steady dipolar solutions are plausible (Parker 1970; p. 399; see also the review of Roberts, 1971, p. 171): Consider a dipole field as shown in Fig. 1a. If the rate of rotation is larger in the outer parts of the

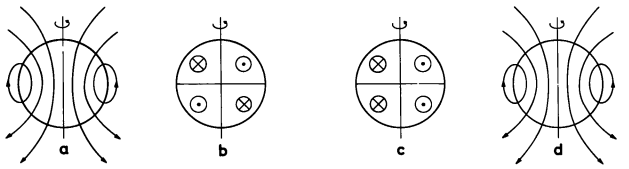

Fig. 1a–d. Steady dynamo action, with $\partial\omega/\partial r>0$ and $\alpha_0>0$. The poloidal field (a) is wound up to produce a toroidal field (b) which, with the help of the α-effect, sets up toroidal currents (c); these reinforce the initial field (d). An encircled dot (cross) indicates a vector pointing out (into) the plane of the paper

sphere, i.e. $\Delta\omega>0$, a toroidal field is generated which points out of the paper on the right-hand side in the northern hemisphere (Fig. 1b). The α-effect is antisymmetric with respect to the equatorial plane; with $\alpha_0>0$, it generates the currents indicated in Fig. 1c. These in turn intensify the original dipole (Fig. 1d). We must however keep in mind that differential rotation and α-effect inevitably induce higher field harmonics; the argument is then no longer conclusive. Indeed, the truncation of all but the first poloidal and toroidal harmonics has led Steenbeck and Krause (1966) to an incorrect steady $\alpha\omega$-dynamo (Roberts, 1972). In Section III we shall demonstrate how the mere variation of the dynamo number P or of the parameters r_1 and r_2 can cause a transition from a steady to an oscillatory mode. Some of the steady fields will be illustrated in Section IV.

Finally, in Section V, we shall discuss whether or not steady solutions of our model have any relevance to the Earth's magnetic field. We shall also check the dependence of our results on the particular choice of the δ-shaped profiles of α and $\partial\omega/\partial r$.

II. Formulation of the Steady Problem

In principle, both oscillatory and steady modes could be derived from the equations given in Paper I. Steady solutions would automatically obtain for $\lambda=0$. However, $\lambda=0$ implies $k=0$, and for $k=0$ our original programme breaks down. Moreover, the equations describing the model are much simpler when only steady solutions are to be investigated; thus, we shall write down these equations once more for the special case $\partial/\partial t=0$. Assuming axial symmetry and using

$$\frac{\partial\omega}{\partial r}=\Delta\omega\delta(r-r_1) \tag{1}$$

and

$$\alpha=\alpha_0\cos\theta\delta(r-r_2) \tag{2}$$

[I, Eqs. (1) and (2)], we find the basic equations for A and B, the φ-components of the vector potential and magnetic field, viz.

$$\Delta_1 A+\delta(x-x_2)B\cos\theta=0, \tag{3}$$

$$\Delta_1 B+P\delta(x-x_1)\frac{\partial}{\partial\theta}(A\sin\theta)=0, \tag{4}$$

where[1])

$$\Delta_1=\Delta-\frac{1}{x^2\sin^2\theta} \tag{5}$$

and

$$P=\frac{\alpha_0}{\eta}\frac{\Delta\omega R^2}{\eta}. \tag{6}$$

We have introduced a non-dimensional radial coordinate $x=r/R$. Note that α_0 in Eq. (2) has the dimension of a diffusivity; thus the α-effect magnetic Reynolds number in our model is $R_\alpha=\alpha_0/\eta$ (in the general discussion of Section V, however, we treat α_0 again as a velocity). Except for the spherical surfaces defined by $x=x_1$ and $x=x_2$ the functions A and B satisfy the equation

$$\Delta_1 f=0. \tag{7}$$

The solutions of (7) are

$$x^n P_n^1(\cos\theta) \quad\text{and}\quad x^{-n-1}P_n^1(\cos\theta), \tag{8}$$

where n is a positive integer and P_n^1 is an associated Legendre function. The boundary conditions at $x=0$ and $x=1$, and the jump conditions at $x=x_1$ and $x=x_2$ are exactly the same as in Paper I. Since the latter cause the coupling of different spherical harmonics, none of the elementary solutions (8) alone solves Eqs. (3) and (4). Instead, A and B are expressions of the form

$$A=\sum_{n=1}^{\infty}A_n x^{-n-1}P_n^1(\cos\theta) \qquad x\geqq 1, \tag{9}$$

$$A=\sum_{n=1}^{\infty}(B_n x^n+C_n x^{-n-1})P_n^1(\cos\theta) \qquad 1\geqq x\geqq x_2, \tag{10}$$

$$A=\sum_{n=1}^{\infty}D_n x^n P_n^1(\cos\theta) \qquad x_2\geqq x\geqq 0, \tag{11}$$

and

$$B=0 \qquad x\geqq 1, \tag{12}$$

$$B=\sum_{n=1}^{\infty}(F_n x^n+G_n x^{-n-1})P_n^1(\cos\theta) \qquad 1\geqq x\geqq x_1, \tag{13}$$

$$B=\sum_{n=1}^{\infty}H_n x^n P_n^1(\cos\theta) \qquad x_1\geqq x\geqq 0. \tag{14}$$

Expresions (10), (11), (13) and (14) already satisfy the boundary conditions at $x=0$ and the conditions that A

[1]) This operator was denoted Δ in paper I. In order to avoid confusion with the Laplacian we now prefer the notation Δ_1.

and B and their derivatives shall be continuous at $x=x_1$ and $x=x_2$ respectively.

When eliminating the constants A_n, B_n... we should distinguish the cases $x_1<x_2$ and $x_1>x_2$. The jump conditions, which were derived in Paper I [Eqs. (6) and (7)] under the assumption $x_1<x_2$, would enter the calculation in a different form in the case $x_1>x_2$. It is however straightforward to show that the critical P values to be considered below remain unchanged when x_1 and x_2 replace each other. The same is true for P *and* the eigenvalue λ in the instationary case of Paper I. There is a similar (x_1, x_2)-symmetry in Levy's dynamo model (Stix, 1973). However, in both models the field functions A and B differ in the two cases.

Using the boundary conditions at $x=1$ and the conditions that A and B shall be continuous at $x=x_2$ and $x=x_1$ resp., the jump conditions take the form

$$(2n+1)d_n=\frac{z_1^n}{z_2^{n-1}}\cdot\left(\frac{n-1}{2n-1}h_{n-1}+\frac{n+2}{2n+3}h_{n+1}\right), \tag{15}$$

$$(2n+1)h_n=Pz_1^{n+2}(z_2^{-n-1}-z_2^n)\cdot\left(\frac{n(n-1)}{2n-1}d_{n-1}-\frac{(n+1)(n+2)}{2n+3}d_{n+1}\right), \tag{16}$$

where

$$d_n=D_n\begin{cases}x_1^n & x_1<x_2,\\ x_1^{-n-1}x_2^{2n+1} & x_1>x_2,\end{cases} \tag{17}$$

$$h_n=H_n\begin{cases}\dfrac{x_2^n-x_2^{-n-1}}{1-x_1^{-2n-1}} & x_1<x_2,\\ x_2^{n+2}x_1^{-2} & x_1>x_2,\end{cases} \tag{18}$$

and

$$z_1=\min(x_1,x_2),\quad z_2=\max(x_1,x_2). \tag{19}$$

As in Paper I, the infinite system (15) and (16) divides into two subsystems, one for the even (quadrupole-type) and one for the odd (dipole-type) fields. Again, we truncate these subsystems after, say, N equations and search for zeros $P(N)$ of the determinant of the truncated system. When a solution $P(N)$ is found, N is increased until P does no longer depend on N.

The results to be reported in the next Section are obtained either from a programme based on Eqs. (15) to (19) above or from the original programme described in Paper I, depending whether stationary or instationary modes are considered. In all cases the convergence of the eigenvalues with increasing N was established.

III. Eigenvalues

In the case $P=0$, i.e. either $R_\alpha=0$ or $R_\omega=0$ (or both), the only solutions of our model are unsteady; they decay exponentially in time. In the complex k-plane these solutions are characterized by the real positive zeros of the spherical Bessel functions $j_n(x)$. The two possibilities that can occur when $P\neq 0$ are illustrated in Fig. 2. The eigenvalues k can either move along the real axis. If they move towards the left they may eventually reach the origin; we then have a steady solution. This happens for two of the modes shown in Fig. 2 at $P=P_{01}$ and $P=P_{02}$ respectively. The other possibility is that k becomes immediately complex. The growth rate

$$\lambda=-k^2 \tag{20}$$

is then also complex, i.e. the mode is oscillatory. For a sufficiently large P, the field oscillates with constant amplitude; for the quadropole mode shown in Fig. 2 this is the case at $P\approx 4100$.

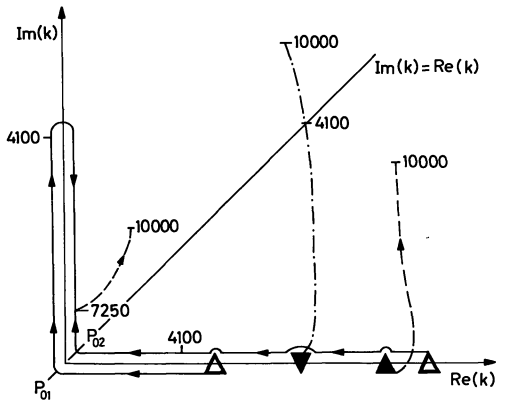

Fig. 2. Complex k-plane, with the (qualitative) position of eigenvalues as functions of P. The open triangles are the simple dipolar decay modes. The full triangles are double decay modes, dipolar upright and quadrupolar inverse. As P increases from zero to positive values, the eigenvalues move either along the axes (exponential modes) or into the complex plane (oscillatory modes)

There is another way to obtain oscillatory solutions: Whenever two exponentially decaying modes "collide" on the real k-axis, or when two exponentially growing modes "collide" on the imaginary k-axis, k will become complex. Thus, in the example shown in Fig. 2, an exponentially growing oscillatory mode is obtained at $P\approx 7250$. But before this can happen one of the exponentially growing modes must reverse its direction: its growth rate *decreases*, in spite of the further *increase* of P. This is an example of "active desctruction", which is typical for non-oscillatory dynamo solutions. Parker (1971) was the first to observe this effect.

We may illustrate the behaviour of the various dynamo modes as functions of P further by means of Figs. 3a–c. The situation of Fig. 2 is depicted in Fig. 3a; in this case the parameters x_1 and x_2 are 0.5 and 0.8 respectively. We see a variety of modes, both exponential and oscillatory. The simplest of all modes, the dipole which decays at a rate π^2 in the case $P=0$, first becomes steady

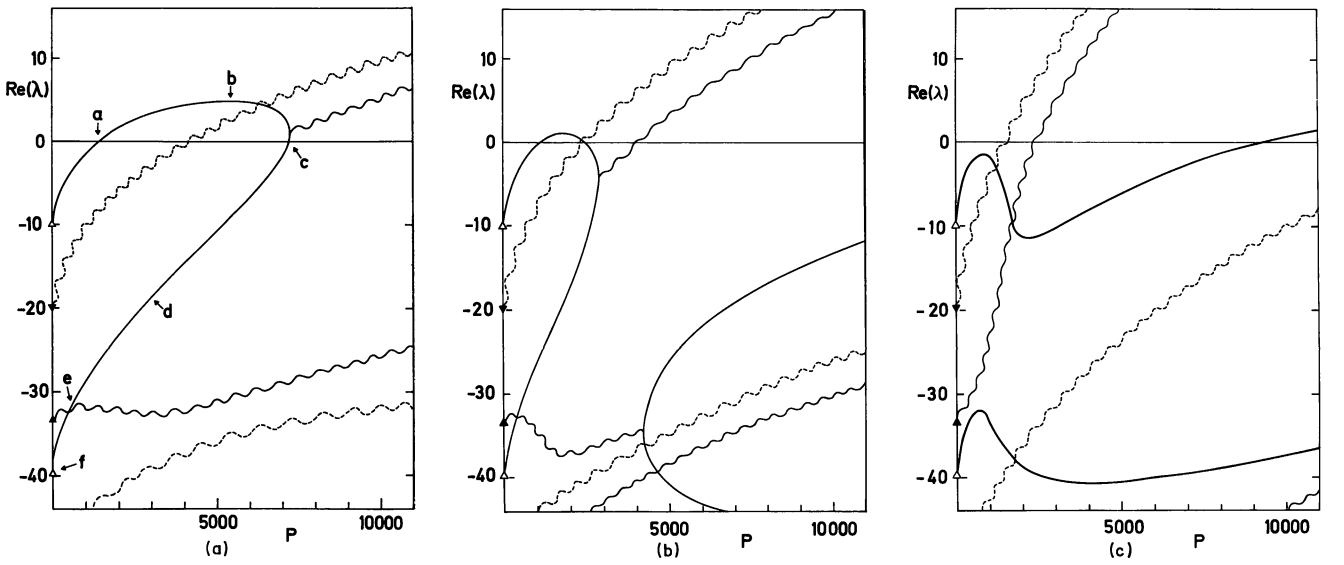

Fig. 3a–c. Growth rates $\mathrm{Re}(\lambda)$ in units of ηR^{-2}, as functions of P, for $x_2 = 0.8$ and $x_1 = 0.5$ (a), $x_1 = 0.55$ (b) and $x_1 = 0.6$ (c); smooth curves = exponential dipole, continuous wavy line = oscillatory dipole, broken wavy line = oscillatory quadrupole. The labels a–f in Fig. 3a mark the eigenvalues of the fields shown in Fig. 7. The triangles are the decay modes, as in Fig. 2

at $P = 1389$ (point a). Its growth rate has a maximum at $P \approx 5400$ (point b) and then decreases to become again steady at $P \approx 7200$ (point c). At $P \approx 7250$ there is a transition into an oscillatory mode. With P that large, however, an oscillatory quadrupole already dominates, i.e. has a larger growth rate. The situation is still similar in Fig. 3b, where only x_1 has been changed from 0.5 to 0.55. We have again the two steady dipole solutions and the oscillatory quadrupole dominating at large P, although the merging of the two exponential dipole modes into the oscillatory dipole now occurs in the region where $\mathrm{Re}(\lambda)$ is negative, i.e. the modes are damped rather than growing. Another transition from oscillatory to exponential modes occurs at $P \approx 4200$, $\mathrm{Re}(\lambda) \approx -35$, but these modes are strongly damped and therefore only of minor importance. The transitions from steady to oscillatory solutions remind us to a very similar behaviour of waves in the Earth's core, where such transitions occur at a critical value of the buoyancy force (Braginskiĭ, 1967).

If x_1 is increased once more by the same amount, a qualitatively different picture obtains. The exponential mode no longer intersects the $\mathrm{Re}(\lambda) = 0$ line and steady solutions only occur at very large P. The oscillatory quadrupole is dominant already for moderate P values.

In principle, we could now repeat the calculations which led to Fig. 3 with different x_2 values. We would obtain similar results. Figure 4 shows the values of the three smallest dynamo numbers P_{01}, P_{02} and P_{03} for which steady solutions exist in the case $x_2 = 0.9$. For x_1 larger than, say, 0.63 the modes at P_{01} and P_{02} disappear; this means that a limiting curve exists in the (x_1, x_2)-plane which seperates the regions of dominating steady dipole and oscillatory quadrupole fields respectively.

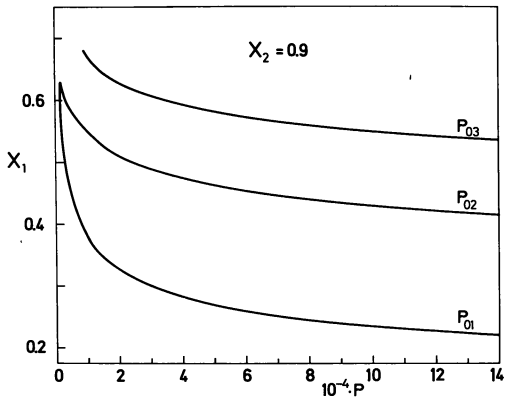

Fig. 4. The x_1 values for which the dynamo numbers P_{01}, P_{02} and P_{03} of the first three steady solutions are marginal, with $x_2 = 0.9$ = constant

So far only the case $P > 0$ has been considered. We have however carried out the calculations also for negative P. The results are similar, although the two most rapidly growing modes are now a steady quadrupole and an oscillatory dipole, depending again on the parameters x_1 and x_2. It has been shown that *no steady quadrupole solution does exist in the case* $P > 0$, and that *no steady dipole solution does exist in the case* $P < 0$. In order to prove this remarkable result, v. Kusserow (1974) showed that the determinants of the truncated systems mentioned in the preceding Section all have a definite sign. A brief outline of this proof is given in Appendix A.

Figures 5a and b are the (x_1, x_2)-planes in the two cases. There is symmetry with respect to the line $x_1 = x_2$; however, the curves of constant P_{01} and P_{02} are drawn only in the upper left halves of the Figures. The limiting

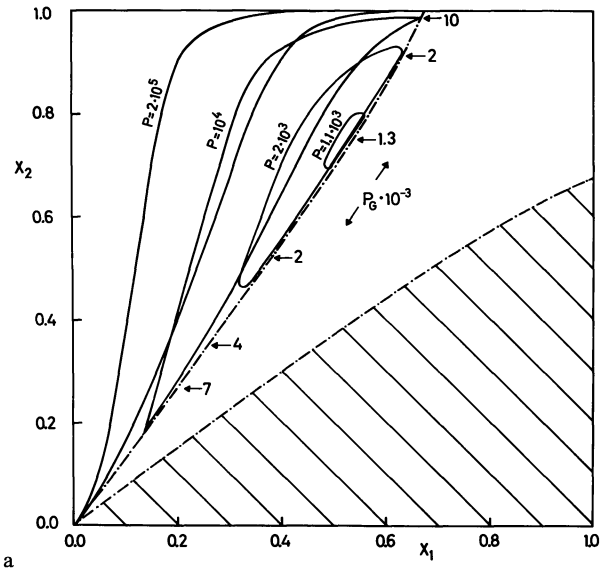

a

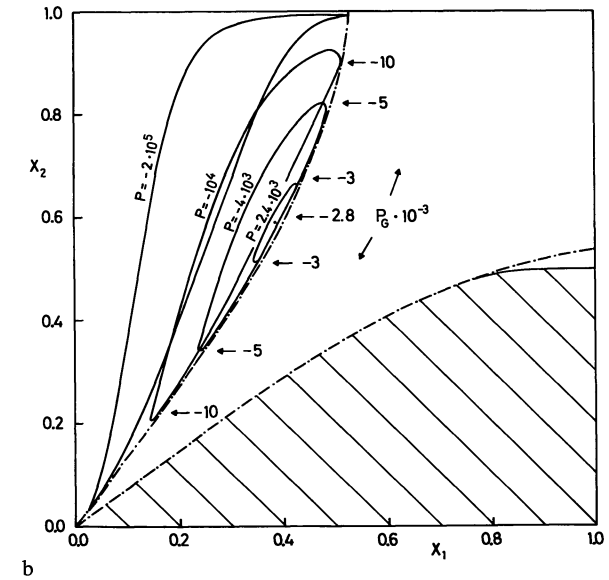

b

Fig. 5a and b. Curves of positive (a) and negative (b) dynamo numbers P for steady dipole (a) and quadrupole (b) solutions in the (x_1, x_2)-parameter space. The hatched region at the lower right has the same contours since the diagram is completely symmetric with respect to the line $x_1 = x_2$. In the regions between the two limiting curves oscillatory modes dominate; this is also the case within the small portion of Fig. 5b around $x_2 \approx 0.5$ and $0.75 \lesssim x_1 < 1$. Some dynamo numbers, P_G, on the limiting curves are given

curve between the regions of oscillatory and steady modes is also drawn in the lower right; there the region of steady modes is simply hatched.

In order to calculate the limiting curve we made use of the fact that P_{01} and P_{02} together form a double solution on this curve (v. Kusserow, 1974). In the case $P>0$ this property indeed defines the true limiting curve as can be seen from Fig. 6a which shows that along the entire curve the value P at which the oscillatory quadrupole is marginal is larger than $P_{01}(=P_{02}\overset{(\mathrm{def})}{=}P_G)$. This is however

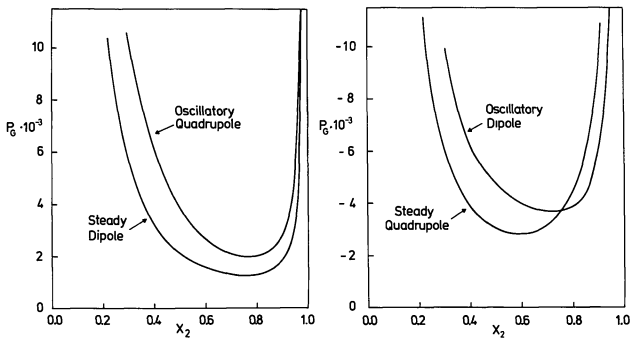

Fig. 6a and b. Dynamo numbers, P_G, on the limiting lines of Fig. 5, as functions of x_2; (a) positive and (b) negative P

not the case when $P<0$. Here the oscillatory dipole dominates even within a part of the region where steady modes at P_{01} and P_{02} are possible. The two curves of Fig. 6b therefore intersect. In Fig. 5b the revised limiting curve is drawn within the lower right half.

Levy (1974) recently pointed out that only half of the steady states are dynamically stable in the sense $\partial \mathrm{Re}(\lambda)/\partial P>0$. This is however not strictly true as the example of our Fig. 3a shows where for *both* P_{01} and P_{02} $\partial \mathrm{Re}(\lambda)/\partial P>0$. On the other hand, the oscillatory quadrupole makes the steady dipole at P_{02} in any case physically uninteresting.

IV. Fields

When the P value for a steady solution is found, or when P and the eigenvalue λ for an oscillatory solution are found, we may arbitrarily choose one of the field coefficients A_n, B_n... and then compute all the other coefficients from the linear and homogeneous system of equations the determinant of which we have set to zero. The field functions A and B are then readily obtained from Eqs. (9) to (14). As usual, we represent the toroidal field by the curves $B(x,\theta) = \text{const.}$ in a meridian (x,θ)-plane. The lines of force of the poloidal field coincide with the curves $A(x,\theta)x\sin\theta = \text{const.}$ and are also shown in the (x,θ)-plane. Since all fields are either symmetric or antisymmetric with respect to the equatorial plane, it is sufficient to show one (the northern) hemisphere. In Figs. 7 and 8 we show several examples, with the toroidal field on the left-hand side and the poloidal field lines on the right-hand side. These two parts of the fields are normalized separately. This is justified since, in contrast to the eigenvalues which depend only on P, the solutions themselves depend on the additional parameter R_α/R_ω; this parameter can be chosen so as to produce a suitable normalization. If, on the other hand, the ratio R_α/R_ω is determined by the physical processes leading to the induction effects, we may simply relable the curves drawn in Figs. 7 and 8.

Figure 7a–f show six field configurations which obtain at various points of the exponential dipolar mode

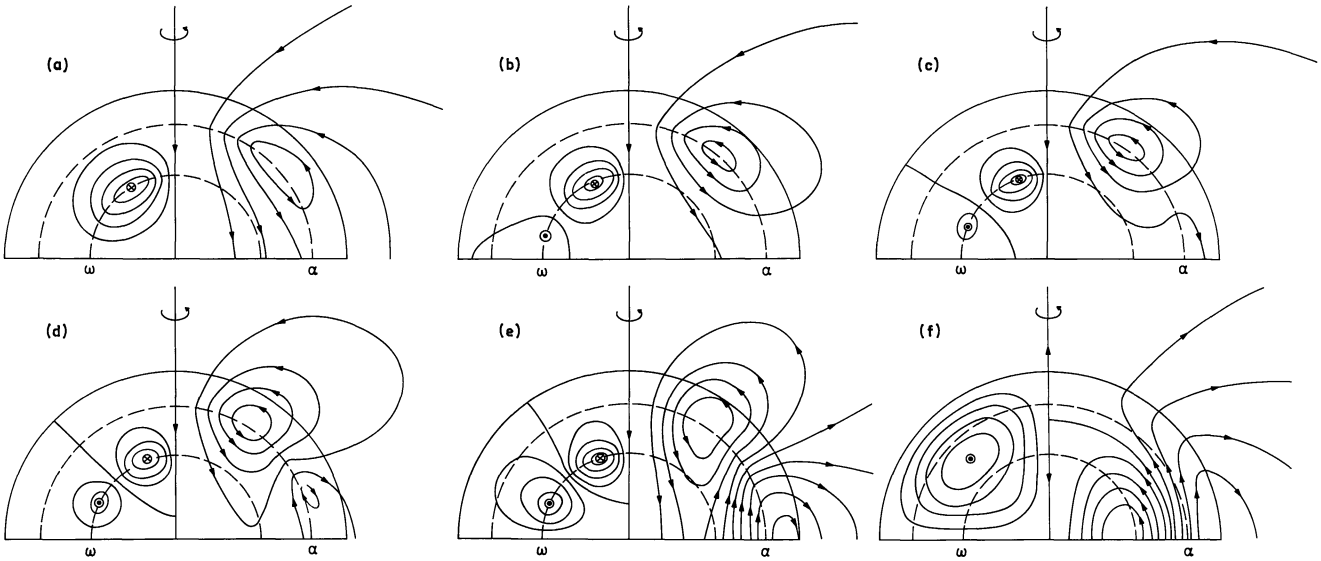

Fig. 7a–f. Meridian sections of dipolar magnetic fields, for the dynamo numbers $P = 1389, 5400, 7198, 3000, 500, 0$, with α_0 and $\Delta\omega$ both positive. The corresponding eigenvalues are marked with labels a–f in Fig. 3a. The right-hand sides show the lines of force of the poloidal field, and curves of constant toroidal field strength are drawn on the left-hand sides. All contours are drawn at equal spacing of the stream function $A \cdot x \cdot \sin\theta$ on the right and the field strength B on the left. Encircled dots and crosses have the same meaning as in Fig. 1. The inner dashed circle indicates the shear surface, the outer indicates the α-effect surface. Only the northern hemisphere is shown; the fields are antisymmetric with respect to the equatorial plane

shown in Fig. 3a ("a" to "f" in that figure). The first (a) is the steady dipole existing at $P_{01} = 1389$. As expected, the toroidal field has its maximum on the shear surface (inner dashed circle), whereas the poloidal field has its 0-type neutral line on the α-surface (outer dashed circle). The dynamo essentially operates as explained in the introduction (Fig. 1), although the presence of field lines closed within one hemisphere indicates that the octupole already plays a role. As P is increased, this octupole becomes stronger, and other harmonics also enter, both into the poloidal and toroidal parts of the fields. Since the dissipation is much faster for higher harmonics, the increase of P does not inevitably lead to a more effective dynamo (in the sense of a larger growth rate). This might be one reason that the growth rate of the considered mode passes through a maximum. Another, and probably more serious reason, is the beginning active destruction which can be illustrated by means of Fig. 7b: The octupole contribution has become so strong that poloidal field lines intersect the shear-surface twice within one hemisphere. Reverse toroidal flux is thus generated; it diffuses towards the α-surface where it helps to destruct the poloidal field. In the second steady state of our mode (Fig. 7c) this destruction, which mainly takes place at low latitude, is just balanced by the original dynamo which is still operating at the higher latitudes; the growth rate is again zero.

The described behaviour of the magnetic field yields an answer to another question concerning $\alpha\omega$-dynamos: Steenbeck and Krause (1969a) have argued that $\alpha\omega$-dynamos should be oscillatory if the induction effects, α and $\Delta\omega$, are spatially separated. But calculations of different authors (Roberts, 1972; Stix, 1973) did not confirm this suggestion. The correct answer to this question probably is that active destruction sets in much sooner (i.e. at smaller P) if the induction effects are not so widely separated in space or more evenly distributed. The effect then prevents the existence of steady states altogether. This interpretation is also suggested by Fig. 1 of Roberts (1972), where the exponential mode always has a negative growth rate, very much like the exponential mode in our Fig. 3c (at small and moderate P values). Zero or positive growth rates are possible only if a wide spatial separation makes the reverse toroidal flux inefficient in its tendency to destruct the field. This is very similar to an argument of Parker (1971, p. 505). On the other hand, oscillatory states *require* reverse toroidal flux; they can therefore more easily operate if α-effect and shear lie chose together or are spatially mixed, or else if P is sufficiently large. This does not, of course, invalidate the fact that the oscillation frequency varies like the inverse square of the distance of the two induction centers (I, Fig. 2). The oscillatory mode emerging from the exponential mode at $P \approx 7250$ has almost exactly the same field geometry as the steady field of Fig. 7c, its oscillation period becomes infinite at the transition point. The field also does not migrate in latitude. Thus, in the vicinity of this transition point, there is little difference between the steady and oscillatory mode. At larger P values, however, the oscillation period becomes comparable with the electromagnetic diffusion time and the field shows the well-known

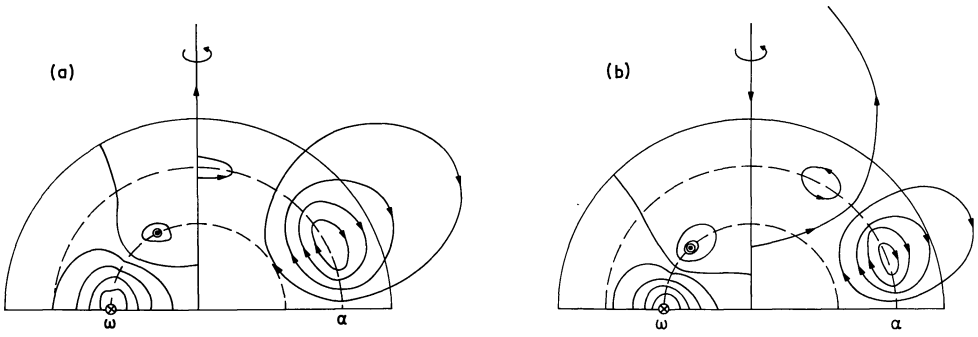

Fig. 8a and b. Meridian sections of quadrupolar steady magnetic fields, with a positive $\Delta\omega$ and a negative α_0, for $P_{01} = -2957$ (a) and $P_{02} = -8525$ (b); $x_1 = 0.45$ and $x_2 = 0.75$ in both cases. See also the description of Fig. 7

latitude migration. This migration is polewards, as well as the migration of the oscillatory quadrupole which is exited above $P \approx 4100$ (in the case $P < 0$ the corresponding dipole migrates equatorwards).

In order to further illustrate the dynamo action we have included into Fig. 7 three fields with negative growth rates, which lie on the lower branch of our exponential mode. The poloidal field shown in Fig. 7f is the mode having one radial node; since $P = 0$, it freely decays at a rate $(2\pi)^2$. This poloidal field is uncoupled from the toroidal "fundamental harmonic" shown on the left-hand side of Fig. 7f. But this situation quickly changes as P increases. Already at the moderate value $P = 500$ (Fig. 7e) the dynamo is very "constructive": as P is increased the growth rate very rapidly increases.

Figure 8 shows the two first steady αω-dynamos for negative P. The case $\alpha_0 < 0$, $\Delta\omega > 0$ is depicted. These fields are quadrupole-type; their maintenance can be made plausible by considerations analogous to those illustrated in Fig. 1. The equatorial toroidal belt and the poloidal field at low latitude are mainly responsible for the dynamo.

V. Conclusions

Does a steady αω-dynamo operate in the Earth's interior? In order to answer this question we must first decide (a) whether there is differential rotation inside the fluid part of the core and (b) whether or not the very complex flow pattern created by the interplay of the buoyancy, Coriolis, Lorentz and inertia forces can be described by a single scalar function, namely α. Then, we may ask whether the concentration of shear and α-effect to two spherical surfaces is realistic in the case of the Earth so that our model is applicable. Or, equivalently, we may ask whether our results seriously change if the δ-functions representing the induction effects in our model are replaced by broader distributions.

Let us begin with the last question. As might be expected from the results of Roberts (1972), there *are* such changes: Figure 9 shows a portion of the (x_1, x_2)-plane with the limiting curves for steady solutions, for several

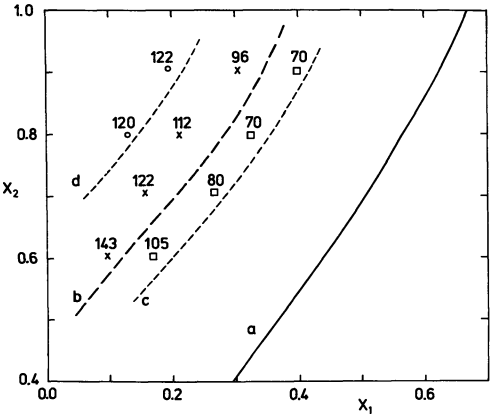

Fig. 9. Limiting curves for steady dipolar solutions of the models described by Eqs. (21) and (22) with (a) $d_1 = d_2 = 0$; (b) $d_1 = d_2 = 0.2$; (c) $d_1 = 0$, $d_2 = 0.2$; (d) $d_1 = 0$, $d_2 = 0.3$. The figures are critical magnetic Reynolds numbers, $P_0^{1/2}$, for the x_1, x_2 values marked with crosses (case b), squares (case c), and circles (case d)

pairs (d_1, d_2), where d_1 and d_2 are the widths of gaussian induction effects, viz.

$$\frac{d\omega}{dx} = \frac{\Delta\omega}{d_1\sqrt{\pi}} \exp\left(-\left(\frac{x - x_1}{d_1}\right)^2\right), \tag{21}$$

$$\alpha = \frac{\alpha_0}{d_2\sqrt{\pi}} \exp\left(\left(\frac{x - x_2}{d_2}\right)^2\right) \cos\theta\,. \tag{22}$$

Eigenvalues of this model were obtained by an expansion method described by Stix (1973). Already for moderate values of d_1 and d_2 the limiting curve moves substantially towards the left, making steady solutions less probable. Thus we conclude that steady αω-dynamos without meridional circulation are possible only if the induction effects, shear and α-effect, are highly concentrated to different parts of the sphere. Probably the spatial separation of the induction effects and meridional circulation (with a proper sign) act in the same way on the field geometry, in the sense that higher harmonics, and thus the reverse toroidal flux, are made less detrimental to steady solutions.

We now turn to the more difficult question whether the α-effect is an adequate description of the regeneration of the poloidal field. Although turbulence in the Earth's core might be caused, for example, by precessional torques (Malkus, 1968), direct observational evidence for such a turbulence is hard to obtain. The irregular structure and variation of the nondipole geomagnetic field indicates that there are irregular fluid motions in the core, having characteristic time scales of decades or longer and a pattern of "continental dimensions" (Roberts and Soward, 1972). Fluctuations of the length of the day also suggest that the characteristic time scale of the core motions is at least several years (Stacey, 1969, p. 39). Let us denote the turbulence inferred from these observations "large scale turbulence", the characteristic parameter being $\ell \approx 10^6$ m and $\tau \approx 10^9$ s. Parker (1969) concluded that fifteen to twenty convection cells should exist in the core and attributed the α-effect (he used the letter Γ) to the helicity of these cells. On the other hand, due to the electric conductivity of the mantle and the attenuating effect of distance, faster time scales and smaller dimensions cannot be detected at the surface. Consistently, Lucke (1959), using quite different arguments, proposed a picture which we shall call "small scale turbulence", with $\ell \approx 10^2 \ldots 10^3$ m and $\tau \approx 10^4$ s. If the latter figures are correct, we have a very large number of convection cells and the theory of the turbulent dynamo is much more appropriate than in the case of only a few cells. Steenbeck and Krause (1969b), using Lucke's data and the formula

$$\alpha = -\frac{16}{15} v^2 \tau^2 \omega . \nabla \ln(\varrho v) \tag{23}$$

derived by Krause (1968), argued that α should change its sign within each hemisphere; for the turbulent velocity, v, vanishes at the inner and outer boundaries of the liquid core and has, therefore, a maximum somewhere in between. In their model the α-effect is a consequence of the preferred (radial) direction defined by the gradient of v; the density, ϱ, is treated as a constant.

Such preferred directions also are necessary in two different approaches: Moffatt (1970) showed that the superposition of random inertial waves having a preferred direction of propagation leads to an α-effect, and Roberts and Soward (1972; see also Braginskiĭ, 1967, 1970) pointed out that MAC waves, where **M**agnetic, **A**rchimedean (buoyancy), and **C**oriolis forces play the dominant roles, also could be responsible for the field regeneration via an α-effect, if there is some asymmetry between the waves propagating in different directions.

The assumption of preferred directions has been criticized by F. H. Busse (1974, private communication). He argued that these assumptions are artificial and, in addition, unnecessary since rotation itself already provides the anisotropy required for dynamo action by means of its ordering effect on the convection. In fact, Rädler (1969, 1970; see also Roberts and Stix, 1971) and Roberts (1972) computed turbulent dynamo models which where based merely on the anisotropy introduced by rotation. These dynamos do not, in contrast to the α-effect dynamos, require lack of mirror symmetry in the turbulence. On the other hand, there is no doubt that on the Sun the radial direction is preferred, due to the density gradient. There this preferred direction leads to an α-effect which, together with differential rotation, very satisfyingly accounts for the oscillatory solar dynamo. Thus, since the α-effect obviously is such an effective means for dynamo action, we think that its application to the Earth is still an attractive idea, although the existence of the necessary preferred directions (either Steenbeck-Krause's gradient of the r.m.s. velocity or an anisotropy of wave propagation) must be regarded as an open question. In this context it is reassuring to know that a completely different approach to the terrestrial dynamo leads to a regeneration term which, with a slightly different definition of $A(r, \theta)$, is equivalent to the α-effect: the expansion of the motion and the field in terms of $\mathcal{R}e^{-1/2}$, where $\mathcal{R}e$ is the magnetic Reynolds number (Braginskiĭ, 1964; Soward, 1972).

The question of non-uniform rotation inside the core is equally difficult. The westward drift of the nondipole field, which amounts approximately to 0.2^0 of longitude per year, seems to indicate that the core rotates at a slightly smaller rate than the mantle (Bullard *et al.*, 1950). According to this view differential rotation would occur in the uppermost layer below the mantle. Braginskiĭ (1967) and Hide (1966), on the other hand, proposed that the westward drift is a manifestation of Alfvén waves which are modified by the Coriolis force, and which travel along the mean toroidal field. But, then, what process but differential rotation should maintain this toroidal field? Let us, therefore, assume that there *is* differential rotation in the core. For its magnitude, $R \cdot \Delta\omega$, we adopt the value 10^{-4} m/s suggested by the westward drift. In this we follow Roberts and Soward (1972).

We must now compare this value of $R\Delta\omega$ with the α_0 derived from Eq. (23). We shall use this equation in a simplified form, so that $\alpha_0 \approx \ell^2\omega/R$, where $R = 3.5 \cdot 10^6$ m and $\omega = 7.3 \cdot 10^{-5}\,\mathrm{s}^{-1}$. In the case of "small scale turbulence" we find $R\Delta\omega \gg \alpha_0$, so that the dynamo is indeed $\alpha\omega$-type (Deinzer *et al.*, 1974). On the other hand "large scale turbulence" leads to $R\Delta\omega \ll \alpha_0$, i.e. an α^2-model, where the α-effect is also responsible for the creation of toroidal flux, would be more appropriate. Paradoxically enough, Steenbeck and Krause (1969b), who employed the "small scale" picture, treated the Earth as an α^2-dynamo, whereas Parker, while arguing in terms of the "large scale" picture, considered it an $\alpha\omega$-dynamo! This situation characteristically reflects our poor understanding of the role of turbulence in the Earth's core. There is however, an *a-posteriori* argument in favour of the $\alpha\omega$- dynamo: If the toroidal field exceeds

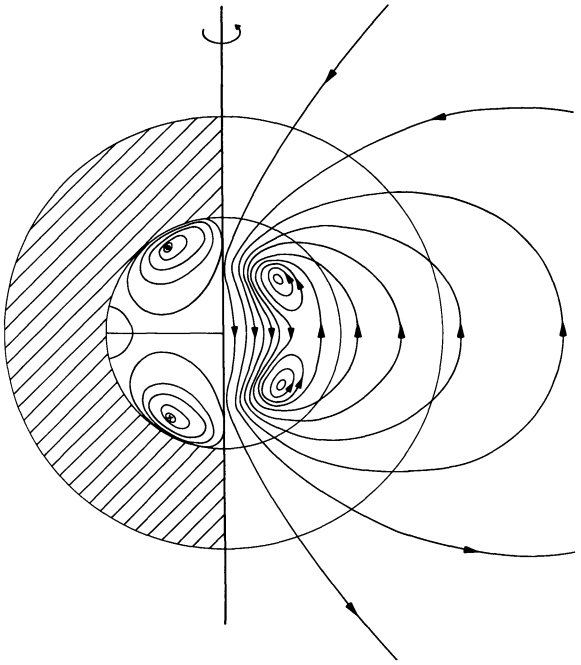

Fig. 10. The Earth as an αω-dynamo, with $x_1 = 0.9$, $x_2 = 0.6$ and $P_{01} = 1558$. On the left the mantle is hatched. See also the description of Fig. 7

the poloidal field by the two orders of magnitude, as suggested by several authors (e.g. Roberts and Soward, 1972), it must be created by a different, and more potent, agent than the poloidal field; as already mentioned, differential rotation is the most plausible candidate.

Notwithstanding all the uncertainties described in the preceding paragraphs we display an example of a steady αω-dynamo (Fig. 10). The parameters x_1 and x_2 are 0.9 and 0.6 respectively. The former is chosen close to unity in order to simulate the differential rotation of Bullard *et al.* (1950). With this value of x_1 we have little choice for x_2. According to Fig. 5a it must not exceed 0.63; on the other hand the existence of the solid inner core allows no α-effect to operate below, say, $x_2 = 0.4$. The dynamo number required for steady dynamo action is $P_{01} = 1558$.

A final speculation pertains to the reversals of the geomagnetic field. Fluctuations in strength or position of the α-effect may occasionally excite an oscillatory mode. If the Earth returns to its "normal" α-effect during a phase of opposite polarity, a new steady field, but with reversed sign, would obtain. This explanation of the field reversals was first proposed by Braginskiĭ (1964b). It is confirmed by the close proximity of steady and oscillatory modes in our model. If the oscillatory state lasts only one half-cycle, the reversal process is essentially that described by Parker (1969) and Levy (1972b).

Appendix A

We shall now prove that our model has no steady dipole solution when $P < 0$. The corresponding theorem, that no steady quadrupole exists when $P > 0$, then follows from analogous considerations.

Let D_n be the determinant of the linear system of Section II, truncated after n equations. D_n has the form

$$\begin{vmatrix} a_{11} & a_{12} & & & & \\ a_{21} & a_{22} & a_{23} & & & \\ & a_{32} & a_{33} & a_{34} & & \\ & & & & & \\ & & & a_{n-1,n-2} & a_{n-1,n-1} & a_{n-1,n} \\ & & & & a_{n,n-1} & a_{nn} \end{vmatrix},$$

where the a_{kj} are defined by Eqs. (15) and (16). Because of the (x_1, x_2)-symmetry mentioned in Section II we may restrict ourselves to the case $x_1 < x_2$. We have

$$D_1 = 3 > 0,$$

$$D_2 = 15 - \frac{2}{5} x_1^5 (x_2^{-3} - x_2^2) P > 0,$$

$$D_3 = 105 - \frac{1}{35} x_1^5 (x_2^{-3} - x_2^2) \cdot \left(98 - 72 \left(\frac{x_1}{x_2}\right)^2\right) P > 0.$$

Now suppose that all determinants D_k with $k \leqq n+1$ are positive. If n is even, we readily see that D_{n+2} is also positive; for, by Eq. (I, 25), we have

$$D_{n+2} = a_{n+2,n+2} D_{n+1} - a_{n+2,n+1} a_{n+1,n+2} D_n > a_{n+2,n+2} D_{n+1} > 0$$

since

$$a_{n+2,n+2} > 0 \quad \text{and} \quad a_{n+2,n+1} a_{n+1,n+2} < 0,$$

as can be seen from the definition of the a_{kj}.

For odd n the product $a_{n+2,n+1} a_{n+1,n+2}$ is positive, so the situation is more complex. Let us, for brevity, introduce

$$a_k = a_{kk},$$

$$A_k = a_{k,k-1} a_{k-1,k},$$

and

$$\Delta D_n = -a_{n+2} A_{n+1} D_{n-1} - A_{n+2} D_n;$$

we then have

$$D_{n+2} = a_{n+2} a_{n+1} D_n + \Delta D_n.$$

From

$$A_{n+2} = P \left(\frac{x_1}{x_2}\right)^{2n+5} (x_2^{2n+5} - x_2^2) \cdot \frac{(n+1)(n+2)(n+3)}{(2n+3)(2n+5)}$$

and

$$A_{n+1} = -P\left(\frac{x_1}{x_2}\right)^{2n+3}(x_2^{2n+5} - x_2^2) \cdot \frac{n(n+1)(n+2)}{(2n+1)(2n+3)}$$

we obtain

$$A_{n+2} = -\left(\frac{x_1}{x_2}\right)^2 f_n A_{n+1}$$

and, therefore,

$$\Delta D_n = A_{n+1}\left(\left(\frac{x_1}{x_2}\right)^2 f_n D_n - (2n+5)D_{n-1}\right),$$

where

$$f_n = \frac{(n+3)(2n+1)}{n(2n+5)}.$$

Since $x_1 < x_2$ and $D_n = a_n D_{n-1} - A_n D_{n-2} < a_n D_{n-1} = (2n+1)D_{n-1}$, we find

$$\left(\frac{x_1}{x_2}\right)^2 f_n D_n - (2n+5)D_{n-1} < f_n D_n - (2n+5)D_{n-1} < (f_n(2n+1) - (2n+5))D_{n-1} = \frac{3-12n-4n^2}{n(2n+5)} D_{n-1} < 0$$

for $n \geqq 2$. A_{n+1} is also negative; hence, ΔD_n is positive, and we obtain the desired result: $D_{n+2} > 0$. Thus, the determinants for all n, odd and even, are positive. No steady dipole solution can therefore exist.

Appendix B

We take this opportunity to correct a number of misprints in the papers of Deinzer and Stix (1971, "Paper I") and Stix (1971).

Paper I:

p. 111, 2nd col., line 13 from below: $\sigma_{\text{eff}}^{-1} = \sigma^{-1} + \beta$. Notice that this β differs from the β introduced by Steenbeck and Krause (1969a) by a factor μ.

p. 112, 2nd col., line 10 from below: $P = \alpha_0 \omega_0 R^2/\eta^2$.

p. 113, 2nd col., line 5: replace "in all higher derivatives" by "of all field components".

p. 113, Eq. (17), right-hand side: $D_n j_n(kx_2)$.

p. 113, Eq. (18), right-hand side: $H_n j_n(kx_1)$.

p. 113, Eq. (19), second term in the { } on the right-hand side: $\frac{n+2}{2n+3}(\ldots)$.

p. 114, 2nd col., after Eq. (25): The limit D does not necessarily exist. But this is not crucial since only the *zeros* of the D_n must converge.

p. 117, 1st col., last line: $|\mathrm{Im}\,\lambda| = 30.7$, $P = -805$ (cf. Stix, 1971, Table 1).

p. 118, 1st col., line 13: $\eta^{-1} = 4\pi \cdot 10^{-8}$ s/m^2.

Stix (1971):

p. 205, 2nd col., line 2 of Section III: $\exp(im\varphi)\ldots$.

p. 205, 2nd col., equations preceding Eqs. (12) and (13):

$$\sum_{n=1}^{\infty}\sum_{m=-n}^{n} e^{\lambda t}\ldots.$$

p. 206, Eq. (17), first term in { } on right-hand side:

$$\frac{(n-1)(n-m)}{2n-1} d_{n-1}^m.$$

p. 208, 1st col., line 15: This result ....

References

Braginskiĭ, S.I. 1964a, *Žh. Èksper. Teoret. Fiz.* **47**, 1084 (= *Soviet Physics* J.E.T.P. **20**, 726)

Braginskiĭ, S.I. 1964b, *Geomag. & Aeron.* **4**, 732; English Transl. p. 572

Braginskiĭ, S.I. 1967, *Geomag. & Aeron.* **7**, 1050; English Transl. p. 851

Braginskiĭ, S.I. 1970, *Geomag. & Aeron.* **10**, 221; English Transl. p. 172

Bullard, E.C., Freeman, C., Gellman, H., Nixon, J. 1950, *Phil. Trans. Roy. Soc. London* A**243**, 67

Deinzer, W., Stix, M. 1971, *Astron. & Astrophys.* **12**, 111

Deinzer, W., v. Kusserow, H.-U., Stix, M. 1974, *Mitt. Astron. Ges.* **34**, 155

Hide, R. 1966, *Phil. Trans. Roy. Soc. London* A**259**, 615

Köhler, H. 1973, *Astron. & Astrophys.* **25**, 467

Krause, F. 1968, Habilitationsschrift, Univ. Jena

v. Kusserow, H.-U. 1974, Diplomarbeit, Univ. Göttingen

Levy, E.H. 1972a, *Astrophys. J.* **171**, 621

Levy, E.H. 1972b, *Astrophys. J.* **171**, 635

Levy, E.H. 1974, *Astrophys. J.* **187**, 361

Lucke, O. 1959, in *Geomagnetismus und Aeronomie*, Vol. 3, p. 313, VEB Deutscher Verlag d. Wissenschaften, Berlin

Malkus, W.V.R. 1968, *Science* **160**, 259

Moffatt, H.K. 1970, *J. Fluid Mech.* **44**, 705

Parker, E.N. 1955, *Astrophys. J.* **122**, 293

Parker, E.N. 1969, *Astrophys. J.* **158**, 815

Parker, E.N. 1970, *Astrophys. J.* **160**, 383

Parker, E.N. 1971, *Astrophys. J.* **164**, 491

Rädler, K.-H. 1969, *Monatsb. Deutsch. Akad. Wiss. Berlin* **11**, 272

Rädler, K.-H. 1970, *Monatsb. Deutsch. Akad. Wiss. Berlin* **12**, 468

Roberts, P.H. 1971, *Lectures in Applied Mathematics*, ed. W.H. Reid, Vol. 14, p. 129. Providence, R.I.: Am. Math. Soc.

Roberts, P.H. 1972, *Phil. Trans. Roy. Soc. London* A**272**, 663

Roberts, P.H., Soward, A.M. 1972, *Ann. Rev. Fluid Mech.* **4**, 117

Roberts, P.H., Stix, M. 1971, *The Turbulent Dynamo.* NCAR Technical Note TN/IA-60

Roberts, P.H., Stix, M. 1972, *Astron. & Astrophys.* **18**, 453

Soward, A.M. 1972, *Phil. Trans. Roy. Soc. London* A**272**, 431

Stacey, F.D. 1969, Physics of the Earth, Space Science Text Series. Wiley, New York

Steenbeck, M., Krause, F. 1966, *Z. Naturforsch.* **21**a, 1285

Steenbeck, M., Krause, F. 1969a, *Astron. Nachr.* **291**, 49

Steenbeck, M., Krause, F. 1969b, *Astron. Nachr.* **291**, 271

Stix, M. 1971, *Astron. & Astrophys.* **13**, 203

Stix, M. 1973, *Astron. & Astrophys.* **24**, 275

W. Deinzer
H.-U. v. Kusserow
M. Stix
Universitäts-Sternwarte
D-3400 Göttingen, Geismarlandstr. 11
Federal Republic of Germany